

DESY SR-78/22
November 1978

DESY-Bibliothek
12. DEZ. 1978

BULK AND SURFACE EXCITONS IN SOLID NEON

by

V. Saile

Sektion Physik der Universität München

E. E. Koch

Deutsches Elektronen-Synchrotron DESY, Hamburg

To be sure that your preprints are promptly included in the
HIGH ENERGY PHYSICS INDEX ,
send them to the following address (if possible by air mail) :

DESY
Bibliothek
Notkestrasse 85
2 Hamburg 52
Germany

BULK AND SURFACE EXCITONS IN SOLID NEON

V. Saile
Sektion Physik der Universität München
8000 München 40, FRG

and

E.E. Koch
Deutsches Elektronen-Synchrotron DESY
2000 Hamburg 52, FRG

Abstract

Transmission and reflection spectra of solid neon in the valence-exciton range ($16 \leq h\nu \leq 22$ eV) have been carefully reinvestigated using highly monochromatized ($\Delta E = 4$ meV) synchrotron radiation. A surface exciton state at $h\nu = 17.15$ eV located 210 meV below the $n = 1$ ($j = 3/2$) bulk exciton is observed and unambiguously identified. Energy positions of the bulk exciton states and line shapes as well as new and more precise values for derived quantities have been determined and are discussed in view of recent theoretical predictions. For the first time we are able to resolve the spin orbit splitting of the $j = 3/2$ and $j = 1/2$ states and study the influence of exchange interaction. The value of 90 meV for the spin orbit splitting is close to the gas phase result. Within a quantum defect approach we evaluate a new band gap of 21.58 eV for solid Ne.

PACS: 71.35 + z, 78.65 Jd

Submitted to Phys. Rev. B

I. Introduction

The onset of electronic absorption in rare gas solids (RGS) is characterized by a number of sharp exciton bands. These excitonic spectra have attracted much interest from both theoreticians and experimentalists. RGS have frequently been regarded as simple prototype substances for insulators due to their simple electronic structure in the ground state with valence bands formed by the outermost closed p-shell electrons and the weak van der Waals forces in the crystal. In spite of this key role there are still conflicting views as how to describe the exciton states in these materials.

The excitation energies E_n of the exciton bands have been mainly described in terms of a hydrogenic Wannier - Mott exciton model¹ based on the effective mass approximation (EMA) and expressed in the well known form

$$E_n = E_G - \frac{B}{n^2} \quad (1)$$

with E_G gap energy, B binding energy and n principle quantum number. The spin orbit splitting of the initial states results in two Rydberg series. For the two $n = 1$ excitons with radii smaller than or close to the nearest neighbour distance the approximations used in a simple Wannier - Mott exciton model are no longer justified. Attempts have been made to calculate these lowest excitation energies by introducing the the so called "central cell corrections"². The most recent theories describe the lowest excitons by the following approaches:

- (i) The lowest excitons can be considered as excitations intermediate between the Wannier - Mott and Frenkel - Peierls³ descriptions. Taking into account the band structure and assuming a localization of electron and hole in the same unit cell, Andreoni et al.^{4,5} applied

an integral equation method to calculate the energy positions, oscillator strengths and the longitudinal - transverse splittings of the first excitons in solid Ar⁴ and Ne⁵. The main drawback of this theory is its limitation to states with electron and hole confined to the same unit cell. An extension to states with $n > 1$ seems to be complicated within an ab initio calculation.

- (ii) Starting from the corresponding atomic transitions $2p^6 + 2p^5 ns, ns'$ in Ne Boursey et al.⁵ calculated the $n = 1$ excitons in solid Ne on the basis of the repulsive - potential curves of the molecular excited states. This theory works very well for the $n = 1$ states but is inadequate for the higher transitions.
- (iii) Resca et al.⁷ described the energy positions of the $n = 1$ excitons for all four rare gas solids within framework of an integral equation approach^{4,5}. In this theory the excitation energy is fixed between the atomic value and the EMA result by a parameter μ/ϵ_{cc} with an effective exciton radius ρ and central cell radius ρ_{cc} . Exploiting the close connection between rare gas atoms and solids, Resca et al.⁸ extended the concept of a quantum defect to the excitonic series. As in atomic theory the space is divided into a sphere around the nucleus and the space outside. The wavefunctions inside the sphere are assumed to be nearly independent of the main quantum number n . By parameterizing the potential inside the atom with the help of the known atomic excitation energies and introducing for the solid the screening of the Coulomb interaction outside the atom Resca et al. obtained agreement with the experimental values for the whole excitonic series for all rare gas solids⁸. In this concept the unknown effective masses of the excitons serve as parameters. This description provides in a very natural way the transition from a Frenkel to a Wannier - Mott picture. On the other hand this approach is semiempirical by exploiting the well know atomic

excitation energies and it yields only energy levels but no oscillator strengths or longitudinal-transverse splittings. A quantum defect theory in the described framework has been applied to solid Ne by Resta⁹.

With the recent observation of surface exciton states in Ar, Kr and Xe and new structures in some of the bulk exciton bands a new challenge has been put forward to further investigate these states experimentally and describe the exciton states theoretically. Several models have been developed to interpret surface excitons in rare gas solids:

- (i) The energy shifts and splittings in environments with different symmetry have been treated by Wolff¹¹ starting from the corresponding atomic excitations. The calculated splittings for localized excitations at the surface of Ar and Kr compare favourably with the experimental results¹².
 - (ii) In the same spirit Chandrasekharan and Boursey¹³ extended their picture described above to excitations in the (100)- and (111)- (111)- surface planes and obtained good values for the excitation energies of surface excitons in all rare gas solids.
 - (iii) Ueba and Ichimura¹⁴ established conditions for the energies of surface excitons relative to the bulk states by a localized perturbation method. In this approach the excitation energies as well as the Davydov splitting is determined by two quantities - the environmental shift term and the exciton transfer term. The application to Ar, Kr, Xe¹⁵ resulted in smaller splittings of the excitation energies than the spin orbit splitting of the initial states¹⁶.
- Solid neon is in principle the most simple insulator with the largest

optically determined band gap of nearly 22 eV. The information about the exciton states as obtained by optical absorption, reflection and energy loss spectroscopy has been reviewed by Sonntag¹⁷. Considering the presently available experimental data for solid Ne, two striking features have to be noted: (i) No spin-orbit splitting of the exciton series could be detected until now in contrast to all other RGS, although Pudewill et al.¹⁸ observed a shoulder in the reflection spectrum from thick ($d \geq 1000 \text{ \AA}$) films on the low energy side of the intense $n = 1$ exciton band separated approximately 0.2 eV from the main peak. It was not clear however whether this splitting could be assigned to the spin orbit splitting. (ii) Surface exciton states have not yet been reported for solid Ne in contrast to all other RGS¹⁰. The only hint for the existence of such a state came from photoemission yield experiments¹⁹ which showed for thin films an extra emission at 17.1 eV well below the $n = 1$ bulk exciton states. This emission was ascribed as possibly being due to excitation of adsorbed single Ne atoms or clusters decaying via energy transfer to the gold substrate and thus leading to an extra photoemission below threshold²⁰.

Thus new experiments were required in order to assess the validity of the above mentioned theoretical approaches and to investigate the "anomalies" of the experimental data in more detail. A careful reinvestigation of the electronic structure seemed also rewarding in view of the increasing interest in the luminescence properties of solid Ne²¹ as well as its properties as a matrix in matrix isolation spectroscopy²².

In the present paper we present and discuss a detailed experimental reinvestigation of the excitonic spectrum of solid Ne. Much more accurate data obtained by high resolution transmission and reflection measurements enabled us to resolve the "anomalies" and observe for the first time the surface exciton states as well as the spin orbit splitting of the bulk exciton states. A preliminary presentation of the reflection data has been given in Ref. 23.

As will be demonstrated in this paper such spectra are difficult to interpret due to the strongly varying optical constants in the excitonic region. Moreover accurate energy positions for strong transitions can be obtained from reflection data only via a Kramers-Kronig analysis. We therefore developed a consistent interpretation especially in the range of the $n = 1$ excitons on the basis of reflection and transmission measurements. It should be noted here that, although the very recent theoretical approaches⁷⁻⁹ used the reflectance data from Ref. 23 without corrections, the general conclusions in these papers are not affected.

After a short description of the experimental arrangement (Sec II) absorption and reflection spectra are presented for several film thicknesses, (Sec III). The spectra as well as derived parameters and the consequences for our present understanding of the exciton states are discussed in Sec IV.

II. Experimental Procedure

Our transmission and reflection experiments have been performed at the synchrotron radiation laboratory at the DESY storage ring DORIS. The apparatus consists of a high-resolution 3m normal-incidence monochromator²⁴, an ultrahigh-vacuum experimental chamber (working pressure 5×10^{-10} Torr after baking) equipped with a He-flow cryostat, a reflectometer and a gas handling system for sample preparation. For the solid state experiments described here we have chosen a medium wavelength resolution of 0.15 \AA ($\approx 4 \text{ meV}$ at 18 eV) over the whole spectral range (300 \AA - 3000 \AA). We note, that this resolution is about 30 times better than the halfwidth of the sharpest structure observed in the spectra. The instrument was calibrated by rare gas absorption lines and provides a reproducibility of 0.1 \AA (2 meV at 17 eV).

The neon samples have been prepared by slow condensation of the sample gas (L'Air-Liquide, purity > 99.995 %) onto the cooled sample holder. The gas handling system was fully bakeable and the purity of the Ne was checked with a mass spectrometer. For the transmission measurements the Ne-gas was condensed onto a LiF substrate coated with sodium salicylate for converting the VUV radiation transmitted through the sample into photons with λ roughly 4000 Å. This long wavelength radiation was measured by a closed EMI 9804 photomultiplier. For the reflectance measurements thin films were prepared in the same manner by condensing the gas on a gold coated LiF crystal. For these measurements the angle of incidence was 7.5°. An open 20-stage electrostatic photomultiplier (Johnston MM2) served as a detector. One major drawback of this technique to measure transmission is its sensitivity to luminescence light emitted by the sample which cannot be distinguished from the transmitted light. On the other hand luminescence doesn't play a role in our reflection geometry with a solid angle of only 6 msterad accepted by the open multiplier. By comparing the data sets measured with both techniques we can estimate the influence of luminescence. It turned out to become important only for thick ($d \gg 100 \text{ Å}$) samples.

The substrate temperatures for condensing the gas have been changed between 6 and 9 K in order to test the influence of substrate temperature on the spectra. Although we observed slight changes in the spectral features all conclusions drawn below are independent of temperature effects.

The measurements have been performed with samples having different thicknesses in order to study also the influence of this parameter. In particular it was possible in this way to discriminate roughly between surface- and volume excitations. The thickness of the films could be determined in principle by observing the changes of the interference in the transparent part of the spectrum below the $n = 1$ exciton with increasing film thickness dur-

ring condensation. For Ne this method gave very poor results since the refractive index is close to 1 in that range of the spectrum¹⁷. Furthermore the technique employed in the transmission experiments using a comparatively rough sodium salicylate substrate prevented us from observing clear interferences. Thus we can only give estimates for the various film thicknesses.

A major consequence of this is the fact that we had to refrain in the present study from determining optical constants. We have plotted for the transmission experiments the optical density, that is $-\ln I(\omega)/I_0(\omega)$ without correcting for the reflectance, where I and I_0 are the transmitted and incident intensities respectively. Thus in the discussion of our results the emphasis is on excitation energies, on the relative intensities of various spectral features and on the line shape of the exciton bands, while the optical constants could not be determined to a better accuracy than previously possible¹⁸.

III. Results

A general view of the optical density of Ne recorded at a temperature of $T = 6 \text{ K}$ appears in Fig. 1. Compared to previous results obtained with lower resolution^{18,25,26} a much more detailed structure in the excitonic region is clearly resolved in this spectrum. Further it is apparent that Ne is almost 100 % transparent in the spectral region above and below the first exciton band. Spectra for the range of the $n = 1$ excitons at around 17.5 eV are shown in more detail in Fig. 2 for a sequence of film thicknesses where $d_0 < d_1 < d_2 < d_3 < d_4$. For very thin films (d_0) we observe one single peak A centered at 16.91 eV. For this film thickness there does not appear any other absorption feature in the whole spectral range $16 \leq h\nu \leq 22 \text{ eV}$. We estimate the thickness d_0 to be equal to one monolayer or even less. Comparing the intensities it is interesting to note that the peak A is quite intense e.g. with respect to the structure observed for d_1 .

When the thickness of the films is increased the peak A disappears and up to 4 features can clearly be discriminated. The peak at 17.15 eV which we have denoted by S is intense for thin films. For thicker samples it's intensity does not increase as rapid as the maxima denoted by $n = 1$ ($3/2$), $n = 1$ ($1/2$) and L ($1/2$). The peak denoted by L appears first as a shoulder (d_2, d_3) and finally develops into a separate maximum for thicker samples.

Turning now to the reflectance data in the same spectral range (Fig. 3) we can identify the same four features in the spectrum obtained for the thickest sample (d_5). They appear almost at the same energies as in the absorption experiment. However, due to the high constant reflectance of the Au-substrate and the weak Ne-absorption outside the exciton bands the situation is more complicated and one observes typical interferences for the vacuum - Ne-film - Au-substrate combination. Thus it is important to follow the changes of the spectra with increasing film thickness from d_1 to d_5 in order to identify the structures correctly. For example, there appears a typical interference minimum between 16.5 eV and 17 eV preceding the first exciton band. This minimum disappears almost completely for the thicker samples, whereas e.g. the structure denoted by S persists for all thicknesses on a strongly varying background. It's also interesting to observe how the reflectance band between 17.5 and 18 eV develops into a broad stop band. Pudewill et al.¹⁸ have measured for this band a reflectance of almost 60 % for thick films with $d \approx 1000 \text{ \AA}$.

In Fig. 4 the optical density as well as the reflectance spectra for a sequence of film thicknesses are displayed for the range $n > 1$. The assignment of the bands is given at the bottom of the figure. Again it is possible to establish a one to one correspondence between the absorption maxima and the features of the reflectance spectra. As already noted by Pudewill et al.¹⁹ one observes a sort of transmission spectra in a reflection geometry for thin

Ne films on a highly reflecting substrate. The reflectance of the Au substrate is attenuated by weak transitions in the rare gas film which are observed as dips in the reflectance spectrum (e.g. for d_1 and d_2). Our new data allow us to follow the changes with increasing absorption of light in the Ne film in detail: Thus e.g. between d_2 and d_3 the dips turn into small peaks until finally for d_4 fully developed reflectance bands are observed for the same energies. We note however that still for d_4 strong contributions from the Ne/Au interface could be observed in the highly transparent region of Ne i.e. below 17 eV (see fig. 3, d_5) and between the $n = 1$ and 2-excitons from about 18.3 eV to 19.8 eV.

Finally in Fig. 5 the results of a surface coverage-experiment are presented. This experiment was performed in order to identify experimentally surface exciton states. Curve A represents the optical density of a clean Ne-sample in the range of the $n = 1$ excitons. Curve B represents the optical density of the same Ne sample coated with a thin Ar-film. The general background is increased since Ar has a smooth but non negligible absorption in this region¹⁷. The most striking observation however is the disappearance of the structure S caused by the coverlayer while the other features remain essentially unchanged. The technique used here and the results and conclusions are similar to the observations for Xe, Kr and Ar in previous experiments¹⁰. Together with the dependence of the absorption upon film thickness as discussed above we take this finding as strong evidence for the fact that the additional maximum S is due to a surface exciton. The difference spectrum normalized to an almost constant Ar-background absorption outside the Ne-exciton bands shows, that the intensity lost in the range of the surface exciton due to the coverlayer is almost equal to the gain for the bulk excitons. Experiments with Xe and Kr coverlayers gave essentially the same results. Further we note that the disappearance of the surface-band can also be observed in the reflectance spectra, although due to additional interference effects with light reflected at the coverlayer - Ne interface admittedly not in such a clear manner²⁷.

IV. Discussion

Several models for the exciton states in solid Ne have been discussed and results of several recent calculations are available^{5,6-9,13} in the literature. In the following we shall try to confront these predictions with the experimental results. A synopsis of the experimentally determined excitation energies appears in table 1, which also gives implicitly our assignments. The energies of the various exciton states are compared to atomic $2p^6 \rightarrow 2p^5 ns, ns'$ transition energies involved with the lowest $2p^6$ electron excitation. In the following discussion we shall first deal with the adsorbate / surface excitations and then turn to the bulk exciton states.

A. Adsorbate state and surface excitons in solid neon

We assign the maximum A observed only for mono- or submonolayers of Ne to an adsorbate resonance. The excitation energy of 16.91 eV is close to the value for the $2p^6 \rightarrow 2p^5 3s, j = 1/2$ state in the gas phase at 16.85 eV^{28,29}. The disappearance of maximum A for thicker samples gives further evidence that the resonance is associated with excited states of adsorbed atoms or of small Ne-clusters which exist prior to the formation of thin coherent Ne-films.

The behaviour of the surface exciton state S observed at 17.15 eV in transmission and 17.12. eV in reflection is quite different, in that it can be observed for the full sequence of film thicknesses. Evidence that this exciton state is confined to the Ne-surface is based on the following observations: (i) The surface exciton is only observed under ultra-high-vacuum conditions. (ii) Upon coating with a different rare gas film the surface exciton disappears (see Fig. 3) and (iii) from the thickness dependence of the surface exciton peak (Fig. 2) where the contribution of the surface exciton remains almost constant, whereas the bulk peaks increase

with increasing film thickness, we estimate that the absorption due to surface excitons is confined to one layer at the sample-vacuum boundary. Such a localization has been experimentally demonstrated for the other RGS³⁰.

For this new state in solid Ne introduced by the presence of the surface we find a FWHM of about 80 meV to 300 meV depending on the sample preparation and background subtraction for deconvolution. These halfwidths exceed considerably those for other RGS where 20 to 30 meV have been observed¹⁰. Two different reasons can be responsible for such a broadening: Either the surface exciton is broadened by the same mechanism which causes a broadening of the bulk $n = 1$ -excitons in solid Ne compared to other RGS (see below) or this surface peak consists of more than one overlapping excitation. As for the second argument it has been shown both experimentally¹⁰ and theoretically¹¹⁻¹³ that three transitions to surface states correspond to the two $n = 1$ bulk excitons in RGS. Due to the small spin-orbit interaction in Ne we expect from an extrapolation of the splittings of surface excitons in Ar and Kr¹⁰ to the case of Ne three states below the $n = 1 (3/2)$ bulk exciton confined to an energy interval of less than 200 meV. Chandrasekharan and Boursy recently calculated the excitation energies for surface excitons in solid Ne¹². On the basis of the molecular excited states derived from the first two atomic excitations and the van der Waals interaction⁶. In this local picture surface excitons are introduced by the different symmetry C_{4v} or C_{3v} compared to the bulk O_h symmetry. Their ab initio calculations yield three states at about 17.30 eV with a splitting of about 150 meV between the first and third peak. Taking into account a natural halfwidths of 80 meV (1/3 of the bulk widths as for the lighter rare gas solids) for the surface excitons this result is consistent with the experimental observation of one rather broad structure at 17.1 eV.

B. Bulk excitons

The excitation energies for the bulk excitons as well as derived parameters are collected in table 1. Our assignments for the bulk exciton states have already been given in the figures. Following previous studies^{16,25,26} they are given in terms of the Wannier-Mott picture. For the first time two series are observed and denoted by $3/2$ and $1/2$ and considerable improvements in the fine structure of the spectra and the accuracy of the data have been possible. Thus we are able to present a new convincing assignment for the observed transitions and extract improved values for the derived quantities.

Values for band the gaps E_G and binding energies B have been evaluated following the traditional concept of a least square fit for the experimental data $n \geq 2$ on the basis of the Wannier formula (eq. 1). In this way the values of $E_G = 21.50$ eV and 21.58 eV for the $j = 3/2$ and $1/2$ series respectively have been obtained. It has been pointed out recently that this approach is inadequate for solid Ne^3+ . Following Resca et al.⁶ and Resta⁹ we introduced in eq. 1 a quantum defect δ by replacing n^2 by $(n + \delta)^2$. Instead of two unknown quantities E_G and B we now deal with three, including δ . In principle δ is a function of the main quantum number n ³¹, but for noninteracting series it is reasonable to assume in a quantum defect theory a constant δ . This is corroborated by the numerical values obtained in Refs. 8,9 and by the theoretical analysis of the atomic data³². With three excitation energies for the excitons $n = 1,2,3$ we are able to extract by numerical methods the three values denoted $E_G^{(2)}$, $B^{(2)}$ and δ in table 1. We note here that this method results in a good fit for all excitons including the $n = 1$ states. The introduction of a quantum defect overcomes the often discussed problems of a transition between Wannier - like excitations and Frenkel - type excitons with decreasing quantum number. With 21.58 eV the band gap coincides with the

ionization limit for the free atom. As for all these extrapolations the accuracy is considerably lower than for the excitation energies involved. Furthermore for the $j = 1/2$ series we have only three states to determine three unknown quantities and it is difficult to accurately extract the value for the $n = 1$ ($1/2$) state: In transmission it is found at 17.50 eV for thin films and 17.53 eV for thick ones after deconvolution of the strongly overlapping L ($1/2$), $n = 1$ ($1/2$) and $n = 1$ ($3/2$) peaks. In reflection we obtained 17.58 eV for $n = 1$ ($1/2$) but no Kramers-Kronig analysis has been performed to calculate the absorption maxima with these data. Due to these reasons the reliability of E_G ($j = 1/2$) is considered to be lower than that of E_G ($j = 3/2$). Our value for the spin-orbit splitting of the Ne 2p states is therefore not the difference of the two gap energies but the splitting of the $n = 3$ - excitons which are not affected by exchange interaction as the states with lower n (see Ref. 5). The value of 0.09 eV coincides within the experimental error of 0.01 eV with the splitting for the ionization limits $2p_{3/2}$ and $2p_{1/2}$ in the atom³³. The extrapolated band gap of (21.58 ± 0.03) eV is slightly less than the value 21.69 eV reported previously¹⁶. The most obvious influence of a quantum defect $\delta > 0$ is found for the binding energies which are increased by about 30 %.

In table 2 we compare our experimental results with recent theoretical predictions. Generally there is good agreement between theory and experiment. Since the higher numbers of the series are rather well described in a hydrogenic like picture for the spread out states the good agreement for $n \geq 2$ is not surprising once the proper value for E_G has been obtained.

This holds also for a quantum defect theory as long as the quantum defect is small compared to 1. The tightly bound lowest $n = 1$ levels are more difficult to describe and pose more serious problems.

A complete theoretical analysis of the exciton states of solid neon has been presented by Andreoni et al.⁵. For the $n = 1$ exciton the main approximation was to assume that the electron and the hole are confined to the same unit cell (one site approximation). This seems justified in view of the small Bohr radii of the $n = 1$ excitons. The results based on the integral equation approach including the band structure appear in table 2. While the theoretical results for the $n = 1$ binding energies are in fair agreement with experiment, the calculated intensity ratio $I(n = 1, 3/2) / I(n = 1, 1/2) = 1 : 50$ is considerably smaller than the experimental one for which we roughly estimate values between $1 : 5$ and $1 : 10$. If we apply our data to the theoretical dependence³ of the intensity ratio and the splitting of the $n = 1$ states (see Table 1) on $\eta = 2(J+D)/\Delta$ where J , D and Δ are the short and long range exchange terms and the spin-orbit splitting respectively, we find for both the splitting of 0.14 eV and the ratio a value $\eta = 1.2 - 1.8$ while the calculations in Ref. 5 yield $\eta = 3.7$. For the states $n \geq 2$ Andreoni et al.⁵ give an estimate for the excitation energies and intensity ratios on the basis of the atomic values and the effective mass approximation eq. (1) with a given B and corrections for electron-hole exchange and spin-orbit splitting. As for the $n = 1$ - excitons we observe in the experiment quite different intensity ratios: For the $n = 2$ - excitons we estimate an experimental ratio $I(n = 2, 3/2) / I(n = 2, 1/2) \approx 1.2$ (s. Fig. 4). Instead of $\eta = 0.8$ (fig. 5 in Ref. 5) we obtain experimentally a smaller exchange interaction $\eta = 0.4$. Obviously the exchange interaction is considerably overestimated in this theory. A similar observation has been found for solid Ar²⁰.

Exploiting ab initio calculations of the potential curves for the molecular 3P and 1P states of neon²³, Boursey et al.⁶ calculated the two $n = 1$ - excitons states in the solid. With a parameter-free calculation they obtained values which are only 140 meV higher in energy than those observed experimentally.

Resca and Rodriguez⁷ calculated in the framework of the integral equation approach the lowest exciton states. With simple trial wave functions which have the proper behaviour for both the EMA and atomic limit and a parameter for the extension of these envelope functions relative to the central cell radii, they obtained a reasonable description for the transition from an atomic to an EMA picture for the $n = 1$ excitons in Ne, Ar, Kr, Xe.

Remarkable progress in describing the whole exciton series for all RGS has been made by a quantum defect theory developed by Resta and Resca et al.^{8,9}. In this semiempirical approach the known atomic binding energies determine the potential inside the atoms in the solid while outside a statically screened Coulomb potential is assumed. For the exciton the true electron mass is assumed inside the atom and outside an effective mass. Thus the close analogy between Rydberg states in rare gas atoms and excitons in rare gas solids is directly exploited. The experimental quantum defect of 0.24 - 0.28 is somewhat smaller than the theoretical one of 0.35 in Ref. 8. These differences in δ are probably the reason why the theoretical excitation energies are too high at low quantum numbers. The atomic values for δ are with approximately 0.7 much higher than those for the solids. An extension of the quantum defect approach to all RGS is found in Ref. 8. The theory is essentially the same as in Ref. 9 but for the fit of the experimental data the effective mass μ is treated as a parameter due to the reason that an effective mass at the bottom of the conduction band is inappropriate for localized states⁸. We compare in table 2 also the various effective masses with the experimental value $\mu = \frac{B \text{ (eV)}}{13.606 \text{ eV}} \cdot n_0^2$ with

$\epsilon_0 = 1.24$.

C. Line shape and longitudinal transverse splitting for the $n = 1$ bulk excitons

The observed line shape for the $n = 1$ excitons (Fig. 2 and 3) is quite complicated and we can only hope to extract qualitative information concerning this point. This complication of the spectrum is due to (i) the strong overlap of surface states with bulk excitons, (ii) the proximity of the $n = 1$ ($3/2$) and $n = 1$ ($1/2$) bulk states (see above) and (iii) the appearance of the feature L on the high energy side of the band which we identify as the excitation of longitudinal exciton states (see below). Nevertheless large widths of the $n = 1$ ($3/2$) and $n = 1$ ($1/2$) peaks in Ne of the order of 200 meV are obtained after deconvolution of the peaks. This value has to be compared with the halfwidths for the $n \geq 2$ exciton states (roughly 100 meV) and the line shape of exciton states in other RGS. For example, the line shape analysis of bulk excitons of Ar, Kr and Xe yields Lorentzians with halfwidths ~ 80 meV²³. Thus according to Toyozawa's model³⁴ the weak exciton-phonon scattering case is realized for these systems. In contrast to this the estimate of roughly 200 meV for the halfwidths in solid Ne is in favour of localized exciton states (strong scattering case) where motional narrowing is not important. We note that the localized nature of the $n = 1$ excitons in solid Ne is also in accord with the current view of exciton dynamics as obtained from luminescence experiments²¹.

We interpret the maximum denoted by L ($1/2$) at 17.75 eV (Fig. 2) as the longitudinal (LO) $n = 1$ ($1/2$) exciton which has its transverse counterpart (TO) at 17.50 eV. Due to the smaller oscillator strength of the $n = 1$ ($3/2$) bulk state the longitudinal - transverse splitting for this transition is expected to be only 4 meV. Bulk excitons in cubic crystals are split by the long range dipole-dipole interaction into longitudinal LO (with \underline{E} parallel to \underline{k} , where

\underline{E} is the electric field vector and \underline{k} the momentum of the exciton) and transverse (TO) (\underline{E} perpendicular to \underline{k}) excitons.³⁵ The observation of the longitudinal bulk excitons is usually restricted to electron energy loss spectroscopy where they show up as maxima in $\text{Im} \frac{1}{\epsilon}$. In fact in such experiments performed for Ne the energy loss peak associated with the $n = 1$ excitons has been observed at 17.74 eV and 17.75 eV^{36,37}. In optical ($\underline{k} \approx 0$) normal incidence transmission experiments the longitudinal excitons normally do not couple to the incident transverse electromagnetic field. However in reflection geometry³⁸ and for rough surfaces¹⁹ optical excitation of longitudinal modes becomes possible. The increase of the longitudinal peak with increasing film thickness (Fig. 2) is most probably due to an increased surface roughness for these films.

Our assignment is supported by the electron loss experiments mentioned above and by the observation of the broad "quasi"-stop band between 17.5 and 18.0 eV in the reflectance from thick films which yields $h\nu_{\text{TO}} \approx 17.5$ eV and $h\nu_{\text{LO}} \approx 17.8$ eV. The numerical value which we deduce for the LO-TO splitting in solid Ne is in very good agreement with the values calculated by Andreoni et al.⁵ and by Boursey et al.¹³ (see table 3.). For solid Ar and Kr Andreoni et al.¹⁰ proposed an explanation for the dip in the reflection stop band between the transverse and longitudinal excitation in terms of spatial dispersion and a dead layer for bulk excitons at the surface. However the existence of such a layer of some ten Å is still an open question. We note in passing that we have studied the excitation of the longitudinal modes in more detail in transmission experiments at nonnormal incidence for thin films of solid Kr⁴¹. In this case the situation is conceptually more favourable since the two ($3/2$) and ($1/2$) $n = 1$ bulk exciton states do not overlap and carry roughly the same oscillator strengths. not overlap and carry roughly the same oscillator strength.

We briefly summarize the result obtained in the previous sections in order to draw some general conclusions:

(a) Results from improved optical transmission and reflection experiments have been presented for thin films of solid Ne. These results are important, in that they resolved the "anomalies" for Ne as compared to the other rare gas solids.

(b) Evidence of an adsorbate induced resonance state close to the excitation energy of the corresponding gas phase transition has been obtained. It would be rewarding to extend these experiments at sub-monolayer coverage under well defined surface conditions in order to eventually follow the gradual transition from isolated Ne atoms to clusters and to bulk Ne films and relate the results to theoretical predictions.

(c) As for Ar, Kr and Xe it was possible to detect and study surface exciton states which are introduced by the presence of the surface and which are spatially confined to a region close to it.

(d) Extensive information has been obtained for the bulk exciton states which can be described optimally by a Rydberg series including a quantum defect, which is lower than theoretically estimated.

The derived parameters are only partly in agreement with theoretical predictions. It was possible to observe the doublet splitting in the exciton lines and to extract the spin orbit splitting of the valence band maxima at the Γ point in the Brillouin zone. Furthermore the influence of electron hole exchange interaction is compared with theoretical data.

(e) Finally for the $n = 1$ excitons the excitation of longitudinal modes has been observed in both transmission and reflection experiments and the nature of these states is briefly discussed.

Thus we believe that with these results and the relation to recent theoretical approaches, which we discuss a full understanding of the static properties of excitons in solid Ne is at hand. Further information related to the clus-

tering and film-formation may come from experiments where the sample parameters can be varied in a controlled manner over a large range. Recent photo-emission experiment from submonolayer rare gas films reveal interesting extra peaks which are not accounted for in the bulk density of states¹². Deeper insight into the nature of the exciton states may also come from investigations of high resolution luminescence where the various states discussed in the present paper can be selectively excited and where differences of their decay mechanisms might further elucidate their dynamical properties.

Acknowledgement

We are very grateful to Dr. W. Andreoni, Prof. G.F. Bassani, and H.W. Wolff for useful discussions and Drs. E. Boursey and V. Chandrasekharan and Profs. Resca and Resta for providing copies of their papers prior to publications. We are also particularly grateful to Prof. W. Steinmann for his continuous interest and support for this project. This work has been supported in part by Bundesministerium für Forschung und Technologie BMFT from funds for Synchrotron Radiation Research.

Table 1

Wannier notation	n	1	2	3	4	5	$E_G^{(1)}$	$B^{(1)}$	$E_G^{(2)}$	$B^{(2)}$	δ	
Surface exciton	T R G	16.91* 17.15 17.12										
$j = 3/2$	T	17.36	20.25	20.94	21.19	21.32	21.50	5.00	21.58	6.93	0.28	
	R	17.36	20.25	20.93	21.19	21.32	±0.03		±0.03			
	G	16.67	19.69	20.57	20.95	21.15	21.57		21.57			
$j = 1/2$	T	17.50	20.36	21.02	~21.29	21.24	21.58	4.90	21.62	6.32	0.24	
	R	17.58	20.36	21.02	~21.29	21.24	±0.04		±0.06	6.67	0.28	
	G	16.85	19.78	20.66	21.04	21.24	21.66		±0.06			
longitudinal exciton	R	~17.75 ~17.78										
δ_1	T	0.14	0.11	0.08			0.09					
	R	0.22	0.11	0.09	0.10							
	G	0.18	0.09	0.09	0.09	0.10	0.10					
δ_1 Splitting	T R	0.25 0.20										

Table 1 Energy positions of excitons in solid neon and derived quantities. All energies are given in eV. The accuracy is better than 0.01 eV for peak positions and 0.03 eV for the derived values unless otherwise noted in text. $E_G^{(1)}$ and $B^{(1)}$ are energy gaps and binding energies derived with the Wannier formula; $E_G^{(2)}$ and $B^{(2)}$ the same values after introducing a quantum defect δ . Δ_i are the splittings between $j = 3/2$ and $1/2$ states. The value in column $E_G^{(1)}$ is the spin orbit splitting of the Ne 2p - levels. LT is the longitudinal transverse splitting. Transmission and reflection data are denoted by T and R respectively while G denotes values for gaseous Ne taken from MOORE's tables (Ref. 28). The peak near 17.8 eV is ascribed to the excitation of a longitudinal exciton which leads to the longitudinal transverse splitting in the last row. The peak at 16.19 eV denoted by an asterix is only observed for extreme thin films having thicknesses in the order of or below one monolayer. For $n = 1$ ($j = 1/2$) and L(1/2) a difference in energy positions between reflection and transmission is observed due to the high oscillator strength of that transition.

Table 2:

Comparison between experimental transition energies for bulk excitons in solid neon and other parameters with theoretical calculations.

$B_1 = E_G - E(n=1)$ are the real binding energies of the $n=1$ -excitons and μ is the effective mass. The other notations are the same as in table

1. All energies are in eV.

From these gap energies we subtracted the theoretical exciton binding energies.

(e) L. Resca, R. Resta and S. Rodríguez, Sol. State. Comm. 26, 849 (1978), and Phys. Rev. B 18, 696 (1978)

J	Experiment		Theory				
	$3/2$	$1/2$	Ref. a	Ref. b	Ref. c	Ref. d	Ref. e
$n=1$	17.36			17.50	17.65	17.75	17.58
		17.50		17.63	17.75	17.85	17.79
2	20.25		19.98			20.32	20.24
		20.36	20.08			20.42	20.35
3	20.94		20.93			20.94	20.91
		21.02	21.13			21.04	21.03
4	21.19		21.25			21.19	21.19
		21.29	21.34			21.29	21.31
5	21.32		21.40			21.31	21.33
			21.50			21.41	21.45
E_G	21.58		21.67			21.55	21.61
		21.62	21.77			21.65	21.73
B_1	4.22		4.16				
		4.12	3.81				
A_{so}	0.09		0.10			0.10	0.12
ξ	0.28					0.35	~0.5
		0.24				0.35	~0.5
μ	0.8		0.8			0.8	0.97
		0.7					

(a) W. Andreoni, F. Perrot and F. Bassani, Phys. Rev. B 14, 3589 (1976).

(b) E. Boursey, M.-C. Castex and V. Chandrasekharan, Phys. Rev. B 16, 2858 (1977)

(c) L. Resca and S. Rodríguez, Phys. Rev. B 17, 3334 (1978)

(d) R. Resta, phys. stat. sol. (b) 86, 627 (1978); gap energies are obtained by a fit of the experimental data Ref. 23 (see also Ref. 27) and A_{so} is the atomic value

Table 3:

Comparison between experimental and calculated energies for the longitudinal-transverse splitting for the $n = 1$ excitons in solid neon.

	Experiment				Theory			
	Optical excitation (a)		electron energy loss (b)		Ref. (c)		Ref. (d)	
J	$3/2$	$1/2$	$3/2$	$1/2$	$3/2$	$1/2$	$3/2$	$1/2$
$n = 1$	-	-	-	-	0.004		0.236	
$n = 1$		0.25		0.25		0.232		0.252

(a) present work

(b) from electron energy loss experiments taking the difference in peak positions from the maximum in the loss spectrum to the maximum of ϵ_2

J. Daniels and P. Krüger, phys. stat. sol. b 43, 659 (1971)

L. Schmidt, Phys. Letters A 36, 87 (1971)

(c) W. Andreoni, F. Perrot and F. Bassani, Phys. Rev. B 14, 3589 (1976)

(d) V. Chandrasekharan and E. Boursey, preprint, submitted to Phys. Rev. B

References

1. R.S. Knox, Theory of Excitons, Academic, New York (1963)
2. J. Hermanson, Phys. Rev. 150, 660 (1966); J. Hermanson and J.C. Phillips, Phys. Rev. 150, 652 (1966); U. Rössler and O. Schütz, phys. stat. sol (b) 56, 483 (1973)
3. A.S. Davydov, Theory of Molecular Excitons, McGraw-Hill, New York (1962)
4. W. Andreoni, M. Altarelli and F. Bassani, Phys. Rev. B 11, 2352 (1975)
5. W. Andreoni, F. Perrot and F. Bassani, Phys. Rev. B 14, 3589 (1976)
6. E. Boursey, M.-C. Castex and V. Chandrasekharan, Phys. Rev. B 16, 2858 (1977)
7. L. Resca and S. Rodriguez, Phys. Rev. B 17, 3334 (1978)
8. L. Resca, R. Resta and S. Rodriguez, Solid State Commun. 26, 849 (1978); Phys. Rev. B 18 696 (1978)
9. R. Resta, phys. stat. sol. (b) 86, 627 (1978)
10. V. Saile, M. Skibowski, W. Steinmann, P. Gürtler, E.E. Koch and A. Kozevnikov, Phys. Rev. Letters 37, 305 (1976)
11. H.W. Wolff, Extended Abstracts, 5th Intern. Conf. on Vacuum Ultraviolet Radiation Physics, Montpellier, Sept. 5-9, 1977, Vol. 1, p. 214
12. V. Saile and H.W. Wolff, Proc. 7th Intern. Vac. Conf. and 3rd Intern. Conf. on Solid Surfaces (Vienna 1977) p. 391
13. V. Chandrasekharan and E. Boursey, preprint 1978, submitted to Phys. Rev. B
14. H. Ueba and S. Ichimura, J. Phys. Soc. Japan 41, 1974 (1976)
15. H. Ueba, J. Phys. Soc. Japan 43, 353 (1977)
16. We want to note here, that H. Ueba apparently misinterpreted Ref. 10: Instead of two spin-orbit split bulk excitons three states at the surface for Ar and Kr had been observed in Ref. 10. Spin-orbit interaction is clearly present but is unable to explain the additional splitting of the $j = 3/2$ excitation at the surface.
17. B. Sonntag, in: Rare Gas Solids, ed. by M.L. Klein and J.A. Venables, Academic Press, New York, (1977) Vol. II, p. 1021

18. D. Pudewill, F.-J. Himpfel, V. Saile, N. Schwentner, M. Skibowski and E.E. Koch, *phys. stat. sol. (b)* 74, 485 (1976)
19. E.E. Koch, V. Saile, N. Schwentner and M. Skibowski, *Chem. Phys. Letters* 28, 562 (1974)
20. For a discussion of the processes involved see e.g.: D. Pudewill, F.-J. Himpfel, V. Saile, N. Schwentner, M. Skibowski, E.E. Koch and J. Jortner, *J. Chem. Phys.* 65, 5226 (1976)
21. See e.g. G. Zimmerer in: Luminescence of Inorganic Solids, ed. by B. Di Bartolo and D. Pacheco, Plenum Press, New York 1978, in press
22. See e.g. B. Meyer, *Ber. Bunsenges. Phys. Chem.* 82, 24 (1978) and references therein
23. V. Saile, W. Steinmann and E.E. Koch, Extended Abstracts of the 5th Intern. Conf. on Vacuum Ultraviolet Radiation Physics, Montpellier, (1977), p. 199
24. V. Saile, P. Gürtler, E.E. Koch, A. Kozevnikov, M. Skibowski and W. Steinmann, *Applied Optics* 15, 2559 (1976)
25. R. Haensel, G. Keitel, E.E. Koch, N. Kosuch and M. Skibowski, *Phys. Rev. Letters* 25, 1281 (1970)
26. E. Boursey, J.V. Ronda and M. Damany, *Phys. Rev. Letters* 25, 1279 (1970)
27. These interference effects suppressed the weak $n=1$ ($3/2$) bulk state (d_5 in fig. 3). Thus on the basis of reflection spectra only, we first tended to interpret this excitation as a surface exciton with a different assignment for the $n=1$ ($1/2$) and L ($1/2$) states as a consequence. Furthermore this interpretation in Ref. 23 was consistent with that of Ref. 18.
28. C.E. Moore, *Nat. Bur. Standards (U.S.), Circular No 467*, 1, 76 (1949)
29. We associate the adsorbate resonance with the $j = 1/2$ state in the gas phase, whose oscillator strength is about 10 times that of the $j = 3/2$ state (W.C. Wiese, M.W. Smith and B.M. Glennan, Atomic Transition Probabilities, Natl. Stand. Ref. Data Ser. 4, US GPO, Washington D.C. 1966, Vol. 1, p. 128)
30. V. Saile, Thesis, Universität München 1976
31. U. Fano, *J. Opt. Soc. Amer.* 65, 979 (1975)
32. A.F. Starace, *J. Phys. B: Atom. Molec. Phys.* 6, 76 (1973)
33. J.S. Cohen and B. Schneider, *J. Chem. Phys.* 61, 3230 (1974); *J. Chem. Phys.* 61, 3240 (1974)
34. Y. Toyozawa, in: Vacuum Ultraviolet Radiation Physics, ed. by E.E. Koch R. Haensel and C. Kunz, Pergamon / Vieweg, Braunschweig 1974, p. 317
35. W.R. Heller and A. Marcus, *Phys. Rev.* 84, 809 (1951)
36. J. Daniels and P. Krüger, *phys. stat. sol. (b)* 43, 659 (1971)
37. L. Schmidt, *Phys. Letters*, 36 A, 87 (1971) and Thesis, Technische Universität Berlin (1972)
38. Analogous to the coupling of light to phonons as described e.g. by M. Bałkanski, in: Optical Properties of Solids, ed. by F. Abeles, North Holland, Amsterdam 1972, p. 529
39. I. Filinski, *phys. stat. sol. (b)* 49, 577 (1972)
40. W. Andreoni, M. De Crescenzi and E. Tosatti, *Solid State Commun.* 26, 425 (1978)
41. V. Saile and E.E. Koch, to be published
42. K. Horn, M. Scheffler and A.M. Bradshaw, *Phys. Rev. Letters*, 41, 822 (1978)

Figure Captions:

Fig. 1 Optical density ($-\ln I/I_0$) of solid neon in the excitonic range of the spectrum. The main features can be grouped into two series split by spin orbit interaction which converge to the bandgap. For the assignment see text.

Fig. 2 A sequence of spectra ($-\ln I/I_0$) for solid neon in the range of the first excitons for increasing film thicknesses d_0 (insert) to d_4 . For the assignment of the various peaks or shoulders see text. Note that d_1 to d_5 are different from the values denoted by the same symbols in the other figures.

Fig. 3 A sequence of reflectance spectra of solid neon in the range of the first excitons for increasing film thicknesses d_1 to d_5 . The assignment of the various features is the same as in Figs. 1 and 2 (see text). Note that d_1 to d_4 are different from the values denoted in by same symbols in the other figures.

Fig. 4 Optical density ($-\ln I/I_0$) of solid neon in the range of the higher excitons $n > 1$ (upper part) and a sequence of reflectance spectra in the same range for increasing film thicknesses d_1 to d_4 (lower part). The assignment of the various features is the same as in Figs. 1,2 and 3 (see text). Note that d_1 to d_4 are different from the values denoted by the same symbols in the other figures.

Fig. 5 Results for a surface coverage experiment for solid neon in the range of the $n = 1$ exciton. Curve A is the optical density ($-\ln I/I_0$) of a clean neon sample. Upon evaporation of a thin Ar coverlayer the

structure denoted by S disappears whereas the band shape of the remaining peak remains unchanged. In the lower part the different spectrum B-A is shown and the smooth and structurless Ar background is indicated by the broken line.

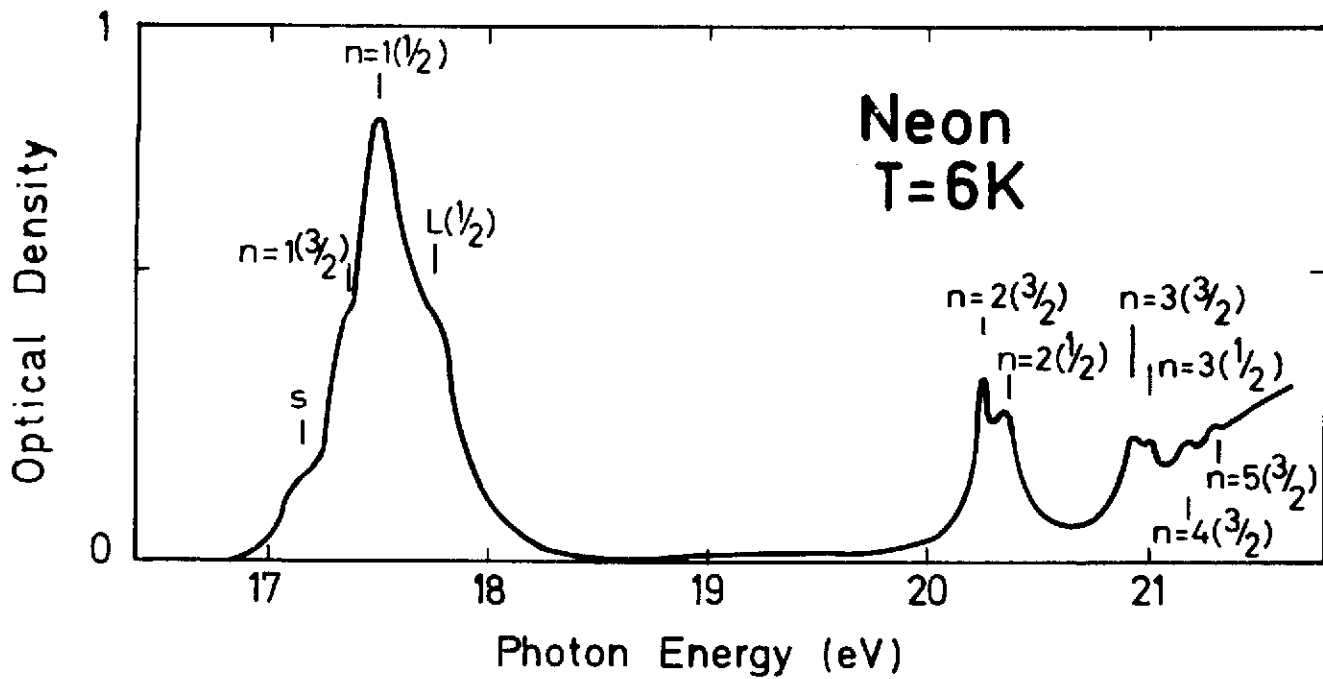


Fig. 1

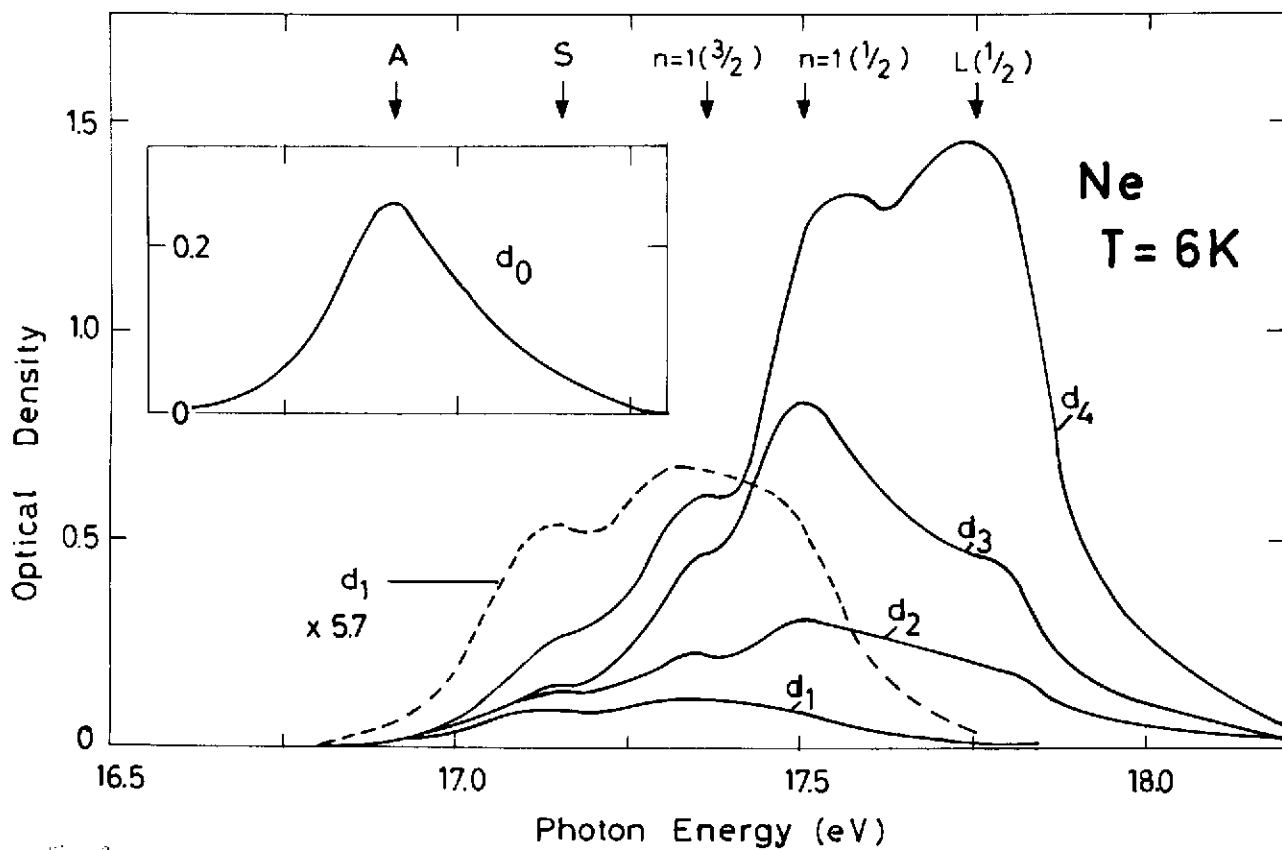


Fig. 2

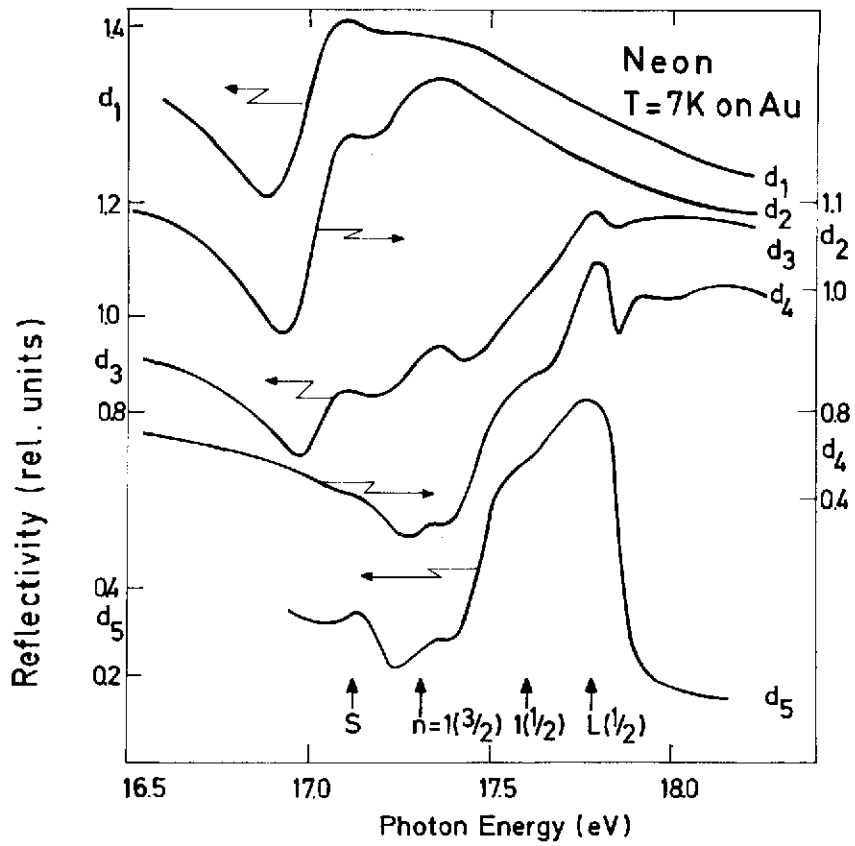


Fig. 3

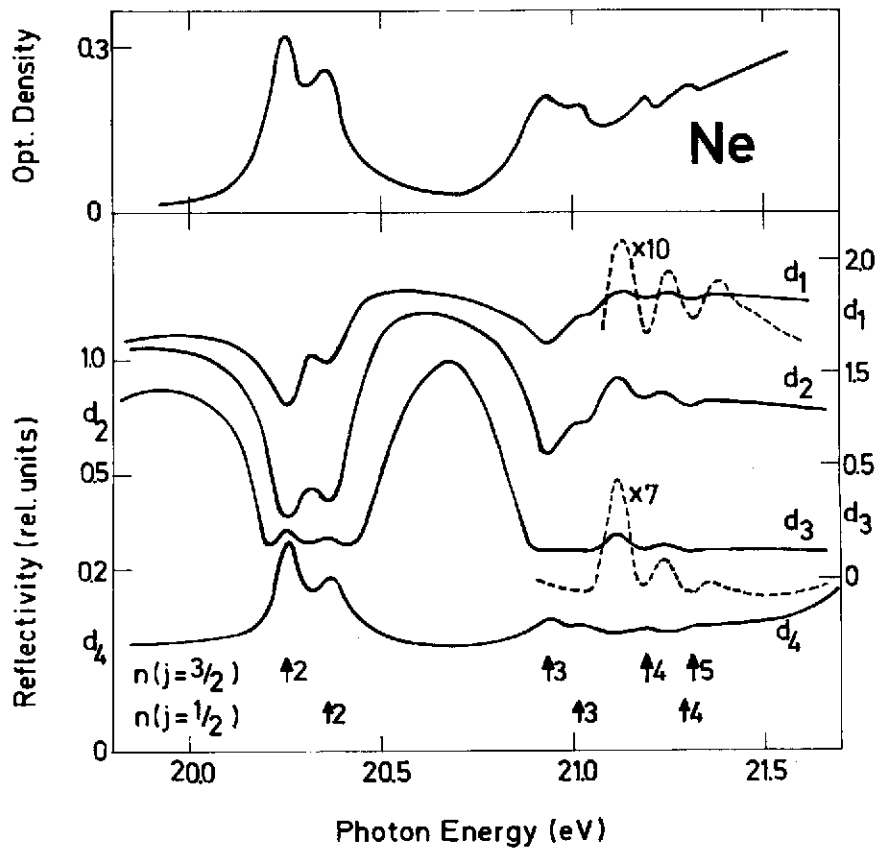


Fig. 4

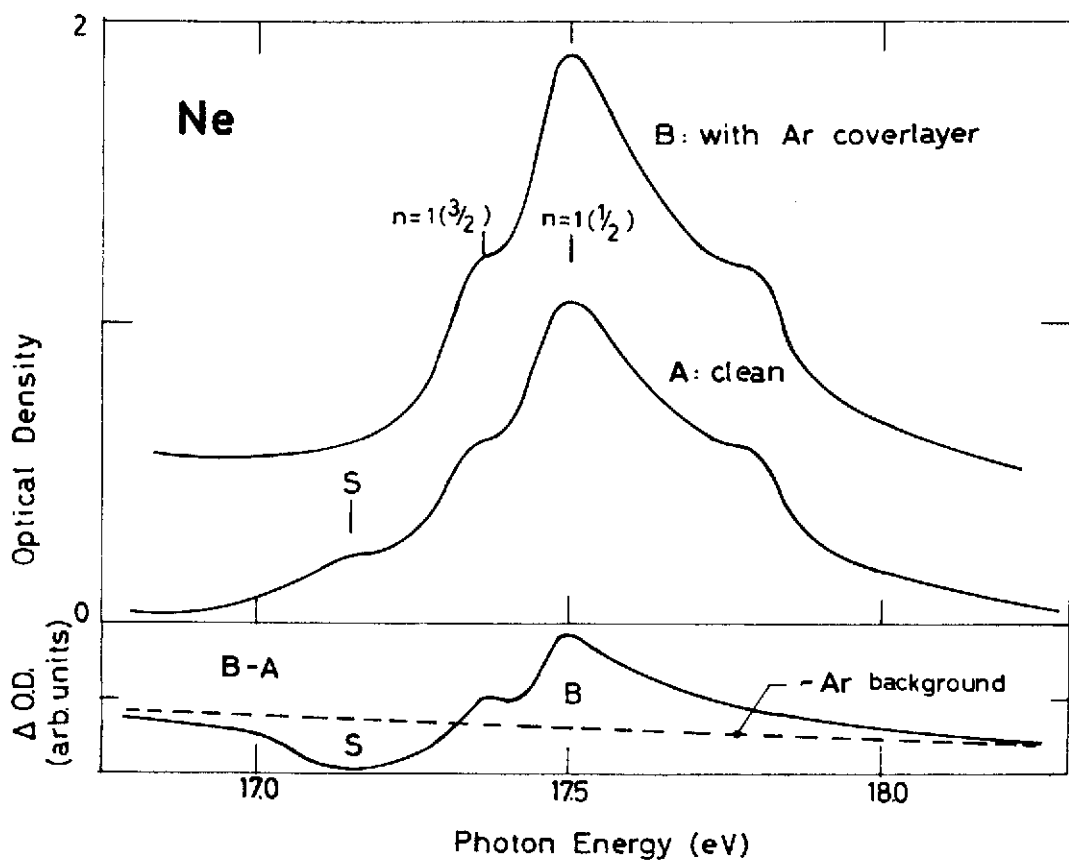


Fig. 5